

AXISYMMETRIC DEFORMATION OF PLATES AND SHELLS WITH PHASE TRANSFORMATIONS UNDER THERMAL CYCLING

L. I. Shkutin

UDC 539.370

A mathematical formulation is given of nonlinear axisymmetric buckling problems for plates and shells in the two-phase zones of austenite-to-martensite transformation. Numerical solutions of the direct- and inverse-transformation problems are used to construct hysteresis loops for thermomechanically cycled, pressure-loaded circular plates and shallow spherical domes of titanium nickelide (NiTi) alloy. It is shown that dynamic instability of the dome deformation process can occur during transformation under loads notably lower than the upper critical values for the isothermal states of the material outside the transformation zone. A theoretical analysis gives external loads below which the dome remains stable in the thermally cycled material with phase transformations.

Key words: *shape-memory alloys, phase transformations, phase strains, thermocycle, interphase hysteresis, plates, shells, buckling, numerical analysis.*

Unlike in [1, 2], in the present study we consider the deformation of thin-walled samples of a shape-memory alloy which undergo phase transformations under thermal cycling. The phase (structural) strain are introduced here using more general (compared to [1, 2]) micromechanical constitutive relations proposed and validated in [3, 4]. The nonlinear thermomechanical problems considered below are formulated assuming that the interphase stress rate is lower than the phase strain rate and ignoring the effect of the variable stress on the phase composition of the alloy (in the uncoupled formulation of [5]). As a result, the direct and inverse phase transformations in the samples are modeled by nonlinear boundary-value thermoelastic problems with an implicit temperature dependence (using a phase parameter which simulates the volume fraction of new-phase crystals).

Micromechanical Constitutive Relations. To establish the stress–strain relation in the direct phase transformation interval, we use the following system of micromechanical constitutive relations, which is more general compared to [1, 2]:

$$\begin{aligned} w_{11} &= \phi_{11} + (S_{11} - \nu S_{22})/E \quad (1 \rightleftharpoons 2), & w_{13} &= \phi_{13} + S_{13}/G, \\ \frac{d\phi_{ii}}{dq} &= (1 - q)^\lambda \left(\varkappa \phi_{ii} + \frac{\tilde{S}_{ii}}{\sigma} \right), & \frac{d\phi_{13}}{dq} &= (1 - q)^\lambda \left(\varkappa \phi_{13} + \frac{S_{13}}{\sigma} \right), \\ q &= \sin \left(\frac{\pi}{2} \frac{T_+ - T}{T_+ - T_-} \right), & T_- &\leq T \leq T_+. \end{aligned} \quad (1)$$

Here w_{iJ} and ϕ_{iJ} are the total and phase strains, respectively, S_{iJ} and \tilde{S}_{ii} are the stress-tensor and stress-deviator components, E and G are the tensile-compressive and shear elastic moduli, ν is Poisson ratio, \varkappa , λ , and σ are the experimental constants of the alloy in the direct phase transformation interval, T_+ and T_- are the initial and final temperatures of the direct transformation, T is the current temperature, $0 \leq q \leq 1$ is an internal state parameter defined as the volume fraction of the martensite phase, and the notation $1 \rightleftharpoons 2$ indicates the existence of equations and relations obtained from the previous equation or relation by replacing the subscript 1 with the subscript 2, and vice versa.

Institute of Computer Modeling, Siberian Division, Russian Academy of Sciences, Krasnoyarsk 660036; shkutin@icm.krasn.ru. Translated from *Prikladnaya Mekhanika i Tekhnicheskaya Fizika*, Vol. 49, No. 2, pp. 204–210, March–April, 2008. Original article submitted January 23, 2007; revision submitted March 27, 2007.

According to (1), the growth of the phase strain is completed at $q = 1$. These relations were proposed in [3, 4], together with simpler relations corresponding to $\lambda = 0$. Apparently, an alloy with $\lambda > 0$ is a more rigid material than an alloy with $\lambda = 0$. Following [2], the phase transformation is treated as a quasi-static process with temperature uniformly distributed over the sample, so that the parameter q does not depend on coordinates.

In the phase transformation interval, the elastic moduli of the material in (1) are not constant but change from their austenite to martensite values. For the phase transformations considered, these moduli can be represented as the averaged relations

$$E = qE_- + (1 - q)E_+, \quad \nu = q\nu_- + (1 - q)\nu_+, \quad G = E/(2 + 2\nu), \quad (2)$$

where the subscripts minus and plus refer to the martensite and austenite phases, respectively.

Assuming that the stress depends on q much more weakly compared to the phase strain [2], we can find an approximate solution of the differential equations (1):

$$\phi_{11} \simeq \eta \frac{2S_{11} - S_{22}}{3\sigma\kappa}, \quad \phi_{22} \simeq \eta \frac{2S_{22} - S_{11}}{3\sigma\kappa}, \quad \phi_{13} \simeq \eta \frac{S_{13}}{\sigma\kappa}, \quad (3)$$

$$\eta(q) \equiv \exp(\kappa[1 - (1 - q)^{1+\lambda}]/(1 + \lambda)) - 1.$$

In relations (3), the function $\eta(q)$ has a different form than that in relations (8) in [2]. This solution satisfies the following physical conditions: the phase strain is zero in the austenite phase and reaches its maximum value in the martensite phase.

Substitution of (3) into the first three equations of (1) yields the approximate constitutive relations

$$E_0 w_{11} \simeq \eta_1 S_{11} - \eta_2 S_{22}, \quad E_0 w_{22} \simeq \eta_1 S_{22} - \eta_2 S_{11}, \quad E_0 w_{13} \simeq \eta_3 S_{13}, \quad (4)$$

$$\eta_1(q) \equiv \frac{E_0}{E} + \eta \frac{2E_0}{3\sigma_0\kappa_0}, \quad \eta_2(q) \equiv \nu \frac{E_0}{E} + \eta \frac{E_0}{3\sigma_0\kappa_0}, \quad \eta_3(q) \equiv \frac{E_0}{G} + \eta \frac{E_0}{\sigma_0\kappa_0},$$

where E_0 is a constant that has the dimension of stress and which is conveniently identified as E_- or E_+ .

Equations (4) describe a directional phase transformation as thermoelastic deformation with an implicit temperature dependence (through the parameter q).

Formulation of the Complete System of Equations. Axisymmetric deformations are analyzed using the mechanical equations of the nonlinear shell model with independent fields of finite displacements and rotations [2]. The complete system of equations for the unknown functions

$$y_0 = \theta, \quad y_1 = a_2 M_{11} l / H_0, \quad y_2 = r / l, \quad y_3 = z / l, \quad y_4 = a_2 T_1 / (\varepsilon C_0), \quad y_5 = a_2 T_3 / (\varepsilon C_0)$$

is given in [2] [see formulas (12)]. In numerical integration of the system, its solutions are sought for discrete values of q in the interval $0 \leq q \leq 1$. The last equality in (1) relates the parameter q to the temperature of the alloy.

The solutions of the boundary-value problems formulated below were obtained for samples of NiTi (titanium nickelide) alloy assuming the following experimental values of the thermoelastic martensite transformation parameters [6, 7]: $T_- = 23^\circ\text{C}$, $T_+ = 43^\circ\text{C}$, $E_- = 28 \text{ GPa}$, $E_+ = 84 \text{ GPa}$, $E_0 = E_+$, $\sigma_0 = 0.049E_+$, $\kappa_0 = 0.0718$, $\nu_- = 0.48$, and $\nu_+ = 0.33$. The parameter λ was varied in the calculations.

Buckling of a Plate under Uniform Pressure. We consider a simply supported circular plate loaded in the austenite phase by a uniform normal pressure of intensity P . The initial shape of the base surface is defined by parameters $\theta_0 = 0$, $z = 0$, and $r = lt$, where l is the radius of the supporting contour.

We examine the axisymmetric deformation of the plate in the phase-transformation interval. The surface-load components for the system of differential equation are defined by the functions $p_1 = p \sin y_0$, $p_3 = p \cos y_0$, and $q_2 = 0$, where $p = Pl/(\varepsilon C_0)$ is the pressure parameter. The boundary conditions on the supporting contour are

$$y_1(1) = 0, \quad y_2(1) = 1, \text{ and } y_3(1) = 0. \quad (5)$$

At the pole of the plate, the following conditions, formulated in terms of the main unknown functions, must be satisfied:

$$T_{13}(0) = 0, \quad T_{11}(0) - T_{22}(0) = 0, \quad M_{11}(0) - M_{22}(0) = 0 \quad (6)$$

(see [2]).

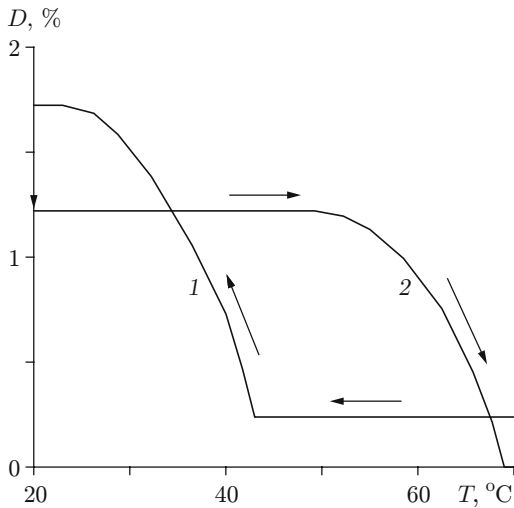


Fig. 1

Fig. 1. Interphase hysteresis for thermomechanically cycled circular plate ($\varepsilon = 0.025$ and $p = 0.01$): 1) direct-transformation trajectory; 2) inverse-transformation trajectory.

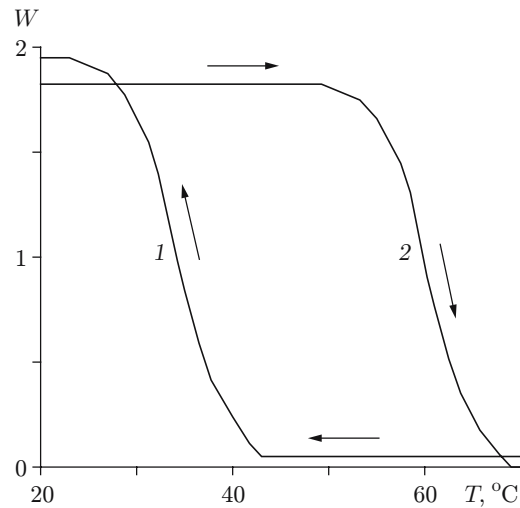


Fig. 2

Fig. 2. Interphase hysteresis for a thermomechanically cycled spherical dome without transient buckling ($\varepsilon = 0.025$ and $p = 0.002$): 1) direct-transformation trajectory; 2) inverse-transformation trajectory.

For the direct martensite transformation interval, the nonlinear boundary-value problem (the system of differential equations (12) in [2] with boundary conditions (5) and (6)) was numerically solved in [2] using the shooting method. To analyze the complete thermocycle, we need to solve the inverse-transformation problem. The solution considered below was obtained as the difference of the solutions of the two boundary-value problems: the direct problem [the system of differential equations (12) in [2] with boundary conditions (5) and (6)] and the pure elastic problem (with no phase strain) with variable elastic moduli (2). Both problems were solved in the interval $0 \leq q \leq 1$ for the same values of the parameters: $\varepsilon = 0.025$, $\lambda = 0$, and $p = 0.01$.

The complete thermocycle obtained by solving the direct- and inverse-transformation problems is shown in Fig. 1 as a curve of the largest strain D (at the plate surface) versus temperature T . For the inverse-transformation interval, the following temperature values were adopted: $T_- = 49^\circ\text{C}$ and $T_+ = 69^\circ\text{C}$ [7]. Curves 1 and 2 in Fig. 1 refer to the direct and inverse processes, respectively. The horizontal portion of curve 1 refers to plate buckling in the austenite phase ($q = 0$) at a pressure $p = 0.01$. Rapid growth of the strain begins and stops during cooling, in the inverse-transformation interval $23^\circ\text{C} \leq T \leq 43^\circ\text{C}$. Load termination at $T_- = 20^\circ\text{C}$ (arrow at the ordinate axis) results in strain reduction due to the vanishing of the elastic component.

The further heating of the unloaded plate (with the acquired phase strain) follows curve 2. Before the beginning of the inverse transformation, the phase strain remains unchanged (the horizontal portion of curve 2), and during the inverse transformation, rapid relaxation of the accumulated stress occurs until the plate assumes the initial (planar) shape.

Buckling of a Spherical Dome under Uniform Pressure. The initial shape of a dome meridian is defined by the parameters

$$r = la_2, \quad z = la_3, \quad \theta_0 = \alpha t,$$

where α is the meridian slope at the support point. The condition of a simply supported dome is formulated with equalities of the form of (5) with $y_2(1) = b/l = \alpha^{-1} \sin \alpha$, where b is the radius of the support contour. Conditions (6) remain unchanged.

Numerical solutions of the direct- and inverse-transformation problems for a dome with the geometrical parameters $\alpha = \pi/36$ and $\varepsilon = 0.025$ and the parameter $\lambda = 0$, are shown in Fig. 2. As in the plate problem, the deformation trajectories of such an asymmetrically strained dome are monotonic in the parameters p and q , all

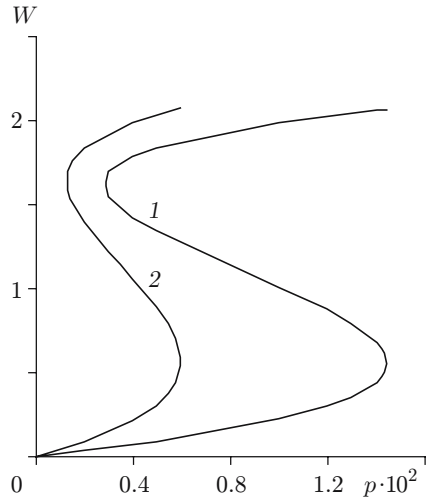


Fig. 3

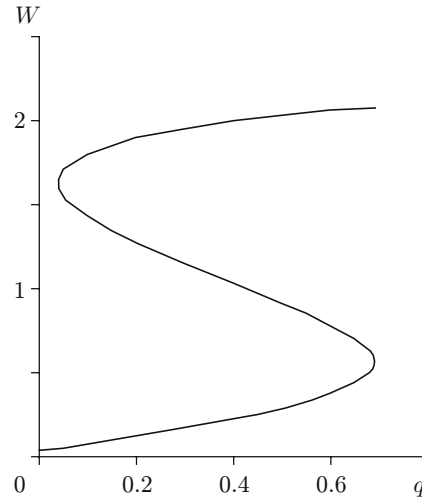


Fig. 4

Fig. 3. Equilibrium-state trajectories of a spherical dome with transient buckling outside the phase-transformation interval: 1) austenite phase ($q = 0$); 2) martensite phase ($q = 1$).

Fig. 4. Equilibrium-state trajectories in the phase-transformation interval ($p = 0.002$).

the equilibrium states being stable, exhibiting no transient buckling [2]. The complete thermocycle for the dome is shown in Fig. 2 as curves of the maximum deflection W (normalized to the dome height) versus temperature T . The direct transformation was calculated for the loading pressure $p = 0.002$. The inverse transformation was calculated assuming no applied load. Figure 2 agrees qualitatively with Fig. 1.

The thermocycle with transient buckling was calculated for a thinner dome with $\alpha = \pi/36$ and $\varepsilon = 0.01$. We first analyzed the isothermal deformation processes observed outside the transformation interval (in the austenite and martensite phases) with variation of the loading parameter. The equilibrium-state trajectories of the dome versus the parameter p are shown in Fig. 3 [curve 1 refers to the austenite phase ($q = 0$) and curve 2 to the martensite phase ($q = 1$)]. Both trajectories are nonmonotonic and have two critical points (p, W): (0.0144, 0.55) and (0.0028, 1.63) are the upper and lower points of trajectory 1, and (0.006, 0.56) and (0.00124, 1.64) are the upper and lower points in trajectory 2.

It should be noted that the curves in Fig. 3 were obtained by solving two pure elastic problems with elastic parameters E_+ and ν_+ (curve 1) and E_- and ν_- (curve 2). The adopted values of the Young moduli differ by a factor of three, and the corresponding values of the upper and lower critical loads by a factor of more than two. At the same time, the critical deflections differ insignificantly.

The equilibrium-state trajectory of the dome versus the parameter q (in the phase-transformation interval for $\lambda = 1$ and $p = 0.002$) is shown in Fig. 4. This trajectory has two critical points (q, W): the upper point (0.69, 0.56) and the lower point (0.04, 1.63). The critical-deflection values are seen to be the same as in the isothermal curves of W versus the parameter p in Fig. 3. The presence of the critical points in the strain trajectories suggests a possibility of abrupt changes in the equilibrium states of the dome.

It should be noted that, for the specified value $p = 0.002$, dome buckling is possible neither in the austenite nor in the martensite phase, but it is observed in the phase-transformation temperature interval. As the parameter p decreases, the upper critical value of q increases: $q = 1$ for $p \simeq 0.0017$. For smaller loading parameters, phase strain is accumulated in the dome without buckling. Thus, the theoretical analysis makes it possible to determine the external loads below which instability of dome deformation does not occur in the phase-transformation interval.

Calculated data for the complete thermocycle are shown in Fig. 5 as curves of the maximum deflection W versus temperature T . The direct transformation process was calculated for the loading-pressure value $p = 0.002$, much smaller than the upper critical loads of the dome in the austenite and martensite phases. The inverse-transformation process was calculated with zero load. The solid curve 1 shows the direct-transformation trajectory

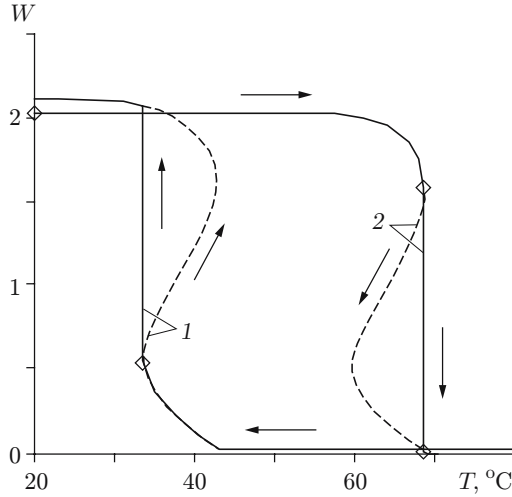


Fig. 5. Interphase hysteresis for a thermomechanically cycled spherical dome with transient buckling ($\varepsilon = 0.01$ and $p = 0.002$): the solid curves are the dynamic hysteresis branches, and the dashed curves are the static hysteresis branches; 1) direct-transformation trajectory; 2) inverse-transformation trajectory.

TABLE 1

q	W	$-\vartheta(1)$	$-\tau_1(1)$	$-s_i(0)$	$(s_3)_{\max}$	$-w_i(0), \%$	$(w_3)_{\max}, \%$
0	0.0335	0.0024	0.9010	2.0202	0.0232	0.0135	0.00062
0.25	0.1433	0.0098	1.0058	2.3505	0.0217	0.0557	0.00176
0.50	0.2899	0.0188	1.1454	2.8956	0.0213	0.1106	0.00277
0.68	0.4984	0.0300	1.3989	4.0485	0.0203	0.1879	0.00326
0.68	0.6222	0.0357	1.5927	5.0327	0.0281	0.2336	0.00451
0.50	0.9104	0.0480	2.2594	8.7404	0.0646	0.3339	0.00840
0.25	1.2165	0.0627	3.7385	17.4250	0.1493	0.4130	0.01212
0.04	1.6129	0.0918	7.6227	46.2170	0.4040	0.4403	0.01437
0.04	1.6530	0.0952	7.2754	46.0360	0.4016	0.4386	0.01428
0.25	1.9257	0.1185	1.5717	17.4240	0.1488	0.4130	0.01342
0.50	2.0301	0.1286	0.5227	10.3420	0.1214	0.3951	0.01578
0.68	2.0750	0.1330	0.2511	8.3241	0.1113	0.3864	0.01785
1.00	2.1230	0.1378	0.0398	6.6667	0.1018	0.3768	0.02153

of the buckled dome with an abrupt jump at the upper critical point ($q \simeq 0.69$ and $T \simeq 33.3^\circ\text{C}$). The solid curve 2 shows is the inverse-transformation trajectory with a sudden jump at the lower critical point ($q \simeq 0.04$ and $T \simeq 68.5^\circ\text{C}$). The solid curves 1 and 2 form the dynamic hysteresis loop for the dome exhibiting instantaneous transitions from one equilibrium shape to another at fixed temperature. It is seen that the loss of stability in a transient buckling mode is possible in both the direct and inverse transformations. The dashed curves 1 and 2 in Fig. 5 form the static hysteresis loop for the phase strain oriented along the equilibrium-state trajectory of the dome (see Fig. 4).

Table 1 shows detailed data illustrating the evolution of the phase strain in the dome at $p = 0.002$. For some values of q , the table gives local values of the deflection W , rotation ϑ , radial-force parameters $\tau_1 = 100T_1/(\varepsilon C_0)$, stresses $s_i = 100S_{ii}/(\varepsilon E_0)$ and $s_3 = 100S_{13}/(\varepsilon E_0)$, and strains $w_i = w_{ii}$ and $w_3 = w_{13}$ [2]. The tangential components of the stress and strain tensors reach the maximum values at the pole of the dome, and the transverse (an order of magnitude lower) components, at the supporting contour and inside the interval. It follows from the table data that the assumption of a low rate of stress changes with the parameter q is not valid in the regions of unstable, overcritical, predominantly flexural strains, and it is valid in the regions of stable subcritical and everted shapes of the dome with prevailing tangential strains. It is these dome shapes that are observed in the case of a dynamically thermocycled dome.

A comparative analysis of the governing equations (4) for $\lambda = 1, 0$ showed that, for the same value of q , the phase strain was notably smaller in an alloy specimen with $\lambda = 1$ than in an alloy specimen with $\lambda = 0$.

The interphase hysteresis curves calculated for the plate and for the dome without transient buckling are similar to those obtained in an experimental study of phase transformations in classical samples of shape-memory alloys [7]. Results of the experimental study of dynamic instability of a shallow dome in the thermocycling interval were reported in [8]. Nonetheless, data required for a quantitative comparison of theoretical and experimental data are lacking from [8]. Movchan [5] proved that if phase transformation proceeds under the action of a constant stress the phase strains in the direct and inverse transformations are identical at the points with the same value of the phase composition parameter. This validates the proposed approximate method for thermocycle analysis under quasi-static stresses.

This work was supported by the Russian Foundation for Basic Research (Grant No. 04-01-00267).

REFERENCES

1. L. I. Shkutin, "Analysis of plane phase strains of rods and plates," *J. Appl. Mech. Tech. Phys.*, **47**, No. 2, 282–288 (2006).
2. L. I. Shkutin, "Analysis of axisymmetric phase strains in plates and shells," *J. Appl. Mech. Tech. Phys.*, **48**, No. 2, 285–291 (2007).
3. A. A. Movchan, "Micromechanical constitutive equations for shape-memory alloys," *Probl. Mashinostr. Nadezh. Mashin*, No. 6, 47–53 (1994).
4. A. A. Movchan, "Choice of transition diagram approximation and model for martensite-crystal vanishing from shape-memory alloys," *Appl. Mech. Tech. Phys.*, **36**, No. 2, 173–181 (1995).
5. A. A. Movchan, "Analytical solution of direct- and inverse-transformation problems for shape-memory alloys," *Izv. Ross. Akad. Nauk, Mekh. Tverd. Tela*, No. 4, 136–144 (1996).
6. A. A. Movchan, "Effect of variable elastic moduli and stresses on the phase composition of shape-memory alloys," *Izv. Ross. Akad. Nauk, Mekh. Tverd. Tela*, No. 1, 79–90 (1998).
7. A. A. Movchan and S. A. Kazarina, "An experimental study of the instability due to thermoelastic phase strains under a compressive stress," *Probl. Mashinostr. Nadezh. Mashin*, No. 6, 82–89 (2002).
8. M. A. Khusainov, "Investigation into the axisymmetric buckling of circular plates," *Zh. Tekh. Fiz.*, **67**, No. 6, 118–120 (1997).